# Vanadium extraction from a magnetite ore using alkaline roasting and acid leaching processes: optimization of parameters by response surface methodology

D. Ghoddocy Nejad[1], M. Taghizadeh[1*] and A.R. Khanchi[2]

*1. Chemical Engineering Department, Babol Noshirvani University of Technology, Babol, Iran*
*2. Nuclear Science and Technology Research Institute, Tehran, Iran*

| Keywords | Abstract |
|---|---|
| *Magnetite Ore* <br><br> *Vanadium* <br><br> *Alkaline Roasting* <br><br> *Acid Leaching* <br><br> *Optimization* | In this work, the alkaline roasting and sulfuric acid leaching processes were employed to extract vanadium from the magnetite ore of Saghand mine in central Iran. The response surface methodology based on the central composite design model was applied to optimize the parameters involved in the processes. The studied roasting parameters were temperature (900-1100 °C), sodium carbonate percentage (30-50 wt%), and time (1-3 h). In addition, the studied leaching factors included temperature (70-90 °C), liquid-to-solid ratio (L/S) (5-20 mL/g), sulfuric acid concentration (2-6 M), and time (3-6 h). Under the optimal conditions, the values for temperature, time, and sodium carbonate amounted to 1010 °C, 2.1 h, and 41 wt%, respectively, for the roasting process, while the values for temperature, L/S, sulfuric acid concentration, and time for the leaching process were estimated to be 85 °C, 12.4 mL/g, 4.25 M, and 4.7 h, respectively. Under these conditions, about 83.8 ± 0.9% of vanadium was leached from the magnetite ore. |

## 1. Introduction

Vanadium is a hard, ductile, and malleable transition metal, which is mainly used in specialty steel alloys such as high-speed tool steels. Vanadium pentoxide, the most famous compound of vanadium, has also found a great deal of applications as a catalyst for the production of sulfuric acid [1]. Vanadium is produced from steel smelter slag, minerals such as titanomagnetite and ilmenite, flue dust of heavy oil or as a by-product of uranium mining. The common grade of vanadium in processed ores is usually less than 2% [2, 3].

The average vanadium concentration in the earth crust is about 150 ppm [4]. However, pure vanadium is not found in nature [5]. Vanadium resources are available in combination with several minerals such as carnotite, roscoelite, france villite, montroseite, and magnetite [6, 7]. The

relative scarcity of economically viable vanadium deposits along with the growing demand for this element has caused the price of vanadium to increase rapidly. Recently, the secondary sources of vanadium have attracted much attention as the most considered extraction resource [8].

A large share of vanadium is extracted from the vanadium-bearing slags or magnetite ores [1]. These vanadium-containing materials can be treated by a great deal of processes such as calcium reduction, roasting/leaching, solvent extraction, and ion exchange for extraction of vanadium either as a pure metal, ferrovanadium, or in the form of vanadium pentoxide and other inorganic vanadium compounds [2, 9]. Recovery of vanadium from secondary resources is carried out through the pyro-metallurgical

✉ *Corresponding author: taghizadeh@nit.ac.ir (M. Taghizadeh).*

and hydro-metallurgical as well as the pyro-hydrometallurgical processes [10].

Among the various pyro-hydrometallurgical processes used or suggested for extraction of vanadium, the most widely applied one is alkaline roasting process with *NaCl* or *Na₂CO₃* followed by water, acid or alkaline leaching. Acid leaching can dissolve water-insoluble roasted materials such as magnesium, calcium, and iron vanadate to extract vanadium [2, 11-15].

In titanomagnetite (i.e. one of the most promising vanadium ores), vanadium is available in the form of trivalent or tetravalent ions. Vanadium is produced from this ore through vanadium pentoxide under the oxidative roasting operation [16]. During the roasting process, several phase changes take place, the most important being magnetite conversion to hematite, which starts from 300 °C and ends at 1300 °C. As a result of this conversion, the vanadium spinels are formed. Studies have shown that magnetite grains are distributed after the separation of vanadium [17]. Some sodium salts such as sodium carbonate produce complex compositions during titanomagnetite roasting. The sodium vanadate complex is an important water-soluble complex of this kind. After oxidation of the ore, trivalent vanadium is converted to pentavalent vanadium, and then it reacts with sodium carbonate (reaction 1) to produce water-soluble sodium metavanadate [17, 18].

$$Na_2CO_3 + V_2O_3 + O_2 \rightarrow 2NaVO_3 + CO_2 \tag{1}$$

Recovery of vanadium from steel refining slag is performed through "slag roasting-acid leaching" and solvent extraction [2]. Acid leaching results in decomposition of vanadium-containing compounds and causes further dissolution of vanadium (reaction 2). The "salt roasting-acid leaching" can bring about the highest extent of vanadium recovery for most types of vanadium-containing feeds.

$$H_2SO_4 + V_2O_5 \leftrightarrow (VO_2)_2SO_4 + H_2O \tag{2}$$

Different researchers have proposed various methods to recover vanadium. Li et al. [19] conducted an oxidation process for a low-grade vanadium slag in the presence of sodium carbonate to form water-soluble sodium vanadates, and dissolved the soluble salts in water (i.e. leaching). Zhu et al. [20] extracted vanadium by coal. In their process, the initial roasting was carried out at 950 °C, followed by leaching with sulfuric acid. They were able to extract about 76% of vanadium. He et al. [21] conducted the roasting process at 850 °C for 3 h, followed by alkaline leaching with sodium hydroxide, and final extraction of vanadium in the form of sodium vanadate; they reported a vanadium extraction efficiency of about 67%. Aarabi-Karasgani et al. [22] roasted the steel plant slag at a temperature of 1000 °C for 2 h using 20% sodium carbonate, followed by sulfuric acid leaching under the conditions of 70 °C, $\frac{L}{S} = \frac{15}{1}$, $H_2SO_4 = 3M$, and 150 min. They finally obtained a vanadium recovery of 95%.

Hydrometallurgical processes that seek for a notable improvement in efficiency are not feasible through the traditional (changing one variable at a time) optimization method. Rather, efficiency improvement is achieved by the design of experiment (DOE) methodology. Compared to genetic algorithms and neural network methods, which require a large number of experiments and consequently consume much energy and time, DOE provides more favorable results with a fewer number of experiments [23-26]. Among DOEs, the response surface methodology (RSM) is the best method for hydrometallurgical processes due to two major reasons: accuracy of the results and determination of the interactions between the effective parameters. To create a second-order model for the response variable in the RSM method, central composite design (CCD) can be used to collect data for fitting the second-order responses. In such a case, the need for complete three-level factorial experiments can be ignored using CCD for an optimization process [27-29].

There are great magnetite ore reservoirs in different regions of central Iran. Based on the latest estimates, there are approximately 1.5 billion tons of magnetite ore. The vanadium-containing ores are impure and mixed with other minerals. The Saghand, Gaz, and Zarand mines are located in the iron-rich zones of Bafq. Saghand ore is

comprised of a noticeable amount of vanadium. According to the estimations, around 150 million tons of magnetite ore are deposited in this mine, which provide 2500-3000 ppm vanadium.

The main objective of this investigation was to optimize the alkaline roasting and sulfuric acid leaching processes of vanadium. The conditions of the two processes were optimized for a high vanadium extraction from magnetite ore (a new ore of Saghand mine in central Iran). Parameters such as temperature, amount of sodium carbonate, and time in the roasting process, and sulfuric acid concentration, temperature, liquid-to-solid ratio (L/S), and time in the leaching process were optimized by means of the RSM method. The chemical and mineralogical characteristics of the new ore (Saghand mine) and the roasted ore one were analyzed by X-ray fluorescence spectroscopy (XRF) and diffraction (XRD). Furthermore, characterization of the leached residues was carried out by the scanning electron microscopy (SEM) and energy dispersive spectroscopy (EDS) analyses.

## 2. Materials and methods
### 2.1. Materials
The sample used in this research work was collected from the Saghand mine in Yazd (Iran). After crushing, the sample was dried at 70 °C to reach a constant weight, and was subsequently ground. It was sieved, and the fraction of powder with a size below 0.1 mm was used for further studies. The mineralogical and chemical analyses of the sample were carried out using a diffraction analyzer (XRD, STOE STADI-MP, Germany) and XRF (Oxford Instruments, ED2000, UK). The results obtained are shown in Figure 1 and Table 1.

In addition, the results of the mineralogical studies of more thin and polished sections of the sample by a polarization optical microscope (Olympus, CX21, China) are presented in Figure 2. According to this figure, the sample contains opaque crystals (mainly magnetite) and talc-carbonate veinlets in the space between them. Sulfuric acid used in the leaching experiments was obtained from Merck, with a purity of 98%. Sodium carbonate salt used in the roasting experiments was 99% pure, supplied from Merck.

**Table 1. Results of XRF analysis of the main composition in the raw ore.**

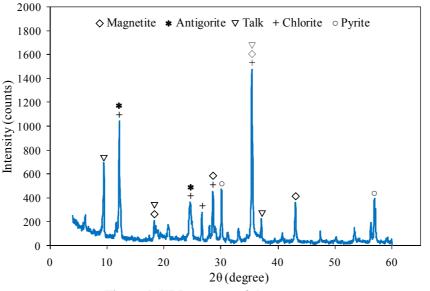| Compound | Wt% |
|---|---|
| MgO | 9.92 |
| $SiO_2$ | 30.85 |
| $SO_3$ | 6.62 |
| $K_2O$ | 0.34 |
| NiO | 0.09 |
| $Sb_2O_3$ | 0.02 |
| U | 0.03 |
| CaO | 0.75 |
| $Fe_2O_3$ | 40.64 |
| $Al_2O_3$ | 3.72 |
| $TiO_2$ | 0.16 |
| $P_2O_5$ | 0.94 |
| $V_2O_5$ | 0.60 |
| LOI | 5.32 |



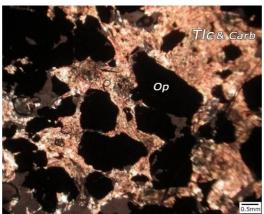**Figure 1. XRD pattern of the raw ore.**

**Figure 2. Mineralogical studies of ore thin and polished sections of the sample (Op = magnetite, TlC = talc and Carb = carbonate).**

## 2.2. Methods
### 2.2.1. Alkaline roasting
Alkaline roasting was carried out to change the vanadium compound to a soluble form. The roasting stage was conducted by placing the sample mixed with certain sodium carbonate (salt) in a muffle furnace at a certain temperature and at a certain time. In this work, according to the results of the experiments, it was found that the optimal roasting conditions were 1000 °C, 2 h, and 40 wt% of sodium carbonate. Figure 3 shows

the XRD pattern of the roasted ore under the optimal conditions.

The range of parameters in the roasting process, which was obtained from the previous studies, is listed in Table 2 [2, 11, 17, 18, 22]. RSM based on CCD was used to evaluate and optimize the effects of temperature, time, and salt content, as the independent variables, on the vanadium recovery.
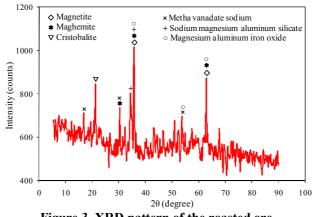


**Figure 3. XRD pattern of the roasted ore.**

**Table 2. Parameter levels and values used in the roasting experimental design.**

| Parameter | Low axial | Low factorial | Center point | High factorial | High axial |
|---|---|---|---|---|---|
| Temperature (°C) | 900 | 940 | 1000 | 1060 | 1100 |
| Time (h) | 1 | 1.4 | 2 | 2.6 | 3 |
| Salt content (wt%) | 30 | 35 | 40 | 45 | 50 |

### 2.2.2. Acid leaching
The roasted sample was leached in sulfuric acid at a certain temperature, liquid-to-solid ratio (L/S), acid concentration, and time within the range obtained from the previous studies (Table 3) [2, 13, 19, 22, 30] in

order to carry out the experimental design using the RSM program.

The leaching experiments were performed at atmospheric pressure in a pyrex reactor equipped with a reflux condenser. The reactor had 3 necks: one for the condenser, one for the thermometer,

and the last neck served for the inlet/withdrawal of samples or pH measurements. The reaction mixture was agitated with a magnetic stirrer and heated on a hot plate indirectly through a water bath. For each leaching test, the sample and a solution with a pre-determined concentration were charged into the reactor, and the mixture was stirred at 300 rpm. After a specific leaching time, a Buchner funnel equipped with a glass filter was used for the filtration. After each experiment, the slurry was filtered and the concentration of

vanadium ions was determined by inductively coupled plasma-optical emission spectrometry (ICP-OES). The measurements were performed using a Perkin Elmer Optima 2000 DV ICP-OES instrument according to ASTM C1109. The calibration range was between 1 and 1000 mg/L. The samples that had concentrations over the standard range were diluted to fall within the range. The operating conditions of the ICP-OES instrument are shown in Table 4.

**Table 3. Parameter levels and values used in the leaching experimental design.**

| Parameter | Low axial | Low factorial | Center point | High factorial | High axial |
|---|---|---|---|---|---|
| Acid concentration (M) | 2 | 3 | 4 | 5 | 6 |
| Temperature (°C) | 70 | 75 | 80 | 85 | 90 |
| L/S (mL/g) | 5 | 8.75 | 12.5 | 16.25 | 20 |
| Time (h) | 3 | 3.75 | 4.5 | 5.25 | 6 |

**Table 4. ICP-OES operational parameters used for the analysis of vanadium.**

| Parameter | Setting |
|---|---|
| Wavelength ($\lambda$) | 292.399 nm |
| RF power | 1400 W |
| Nebulizer | Gemcone |
| Plasma flow | 15 L/min |
| Auxiliary | 0.6 L/min |
| Nebulizer flow | 0.8 L/min |
| Sample flow | 1.0 mL/min |
| Injector | 2.0 mm Alumina |
| Spray chamber | Scott double-pass |

### 2.2.3. Roasting experimental design

An experimental design was used to develop an empirical model to obtain the optimum operating conditions for the roasting process. The optimization procedure was done based on CCD and RSM. RSM applies mathematical and statistical approaches to optimize a response that might be affected by several independent variables and reduces the costs of expensive analysis methods and their associated numerical noises.

To explain the nature of RSM in the optimum region, a five-level central composite design (Table 2) was performed. In general, the central composite design requires a total of ($2^k + 2k + N_0$) runs, where k is the number of factors studied, $2^k$ is the points of the factorial design, 2k is the face-centered points, and $N_0$ is the number of experiments carried out at the center [31]. Duplication of the central points was used to determine the experimental error. In the current work, 8 factorial designs were used and 6 ($N_0 = 6$) central replicates were also employed. As usual,

the experiments were carried out in a random order to minimize the effect of systematic errors. For this purpose, 20 experiments were performed corresponding to the three variables of CCD (Table 5). The parameter levels and the response values (vanadium recovery) are given in Table 5. Each experiment was carried out three times, and the average results of the vanadium recovery evaluation and their corresponding standard deviation values were reported. As it can be seen in this table, the standard deviation values of the results were relatively low and in the range 0.3-1.6%.

The Design-Expert version 8.0.1 software (State-Ease Inc., Minneapolis, MN, USA) was used for the regression and graphical analysis of the data obtained.

### 2.2.4. Leaching experimental design

CCD and RSM were used to optimize the most effective factors and maximize the vanadium extraction. DOE was used to develop an empirical model to obtain the optimum operating conditions of the leaching process. In order to describe the nature of the response surface in the optimum region, a five-level central composite design (Table 3) was performed [32].

Duplication of the central points was used to determine the experimental error. In the current work, 16 factorial designs and 6 central replicates ($N_0 = 6$) were employed, respectively. As usual, the experiments were carried out in a random order to minimize the effect of systematic errors. A total of 30 experiments corresponding to the four

variables of CCD were performed (Table 6). The parameter levels and the respective response values (vanadium recovery) are given in Table 6. Each experiment was conducted three times in the leaching process. The average results of the vanadium recovery evaluation and their corresponding standard deviation values were reported. According to Table 6, the standard deviation values of the results obtained were relatively low and in the range of 0.4-1.9%.

**Table 5. Roasting experimental design; observed response and predicted values.**

| Run No. | Block | Temperature (°C) | Time (h) | Salt content (wt%) | Actual recovery of vanadium (%)[a] | Predicted recovery of vanadium (%) |
|---|---|---|---|---|---|---|
| 1 | Center | 1000.0 | 2.0 | 40.0 | 88.4 ± 0.4 | 86.0 |
| 2 | Fact | 1060.0 | 1.5 | 45.0 | 73.3 ± 0.5 | 74.1 |
| 3 | Axial | 1000.0 | 2.0 | 50.0 | 79.6 ± 1.0 | 78.0 |
| 4 | Fact | 940.0 | 1.5 | 35.0 | 69.1 ± 0.9 | 70.0 |
| 5 | Fact | 1060.0 | 2.5 | 35.0 | 75.0 ± 1.1 | 76.2 |
| 6 | Axial | 1000.0 | 2.0 | 30.0 | 77.6 ± 1.6 | 75.0 |
| 7 | Center | 1000.0 | 2.0 | 40.0 | 83.4 ± 0.7 | 85.1 |
| 8 | Axial | 900.0 | 2.0 | 40.0 | 72.3 ± 0.8 | 71.0 |
| 9 | Axial | 1000.0 | 3.0 | 40.0 | 76.2 ± 0.9 | 75.0 |
| 10 | Fact | 940.0 | 2.5 | 45.0 | 77.1 ± 0.8 | 76.0 |
| 11 | Center | 1000.0 | 2.0 | 40.0 | 85.2 ± 1.0 | 86.0 |
| 12 | Fact | 940.0 | 1.5 | 45.0 | 70.6 ± 1.3 | 73.1 |
| 13 | Axial | 1000.0 | 1.0 | 40.0 | 75.2 ± 0.6 | 73.0 |
| 14 | Axial | 1100.0 | 2.0 | 40.0 | 78.2 ± 0.8 | 76.0 |
| 15 | Center | 1000.0 | 2.0 | 40.0 | 81.6 ± 0.3 | 85.0 |
| 16 | Center | 1000.0 | 2.0 | 40.0 | 88.1 ± 0.9 | 86.0 |
| 17 | Fact | 940.0 | 2.5 | 35.0 | 69.4 ± 0.7 | 71.0 |
| 18 | Fact | 1060.0 | 1.5 | 35.0 | 72.7 ± 0.6 | 75.0 |
| 19 | Fact | 1060.0 | 2.5 | 45.0 | 75.3 ±0.9 | 77.1 |
| 20 | Center | 1000.0 | 2.0 | 40.0 | 86.0 ± 0.8 | 86.0 |

[a]Mean ± standard deviation.

**Table 6. Leaching experimental design; observed response and predicted values.**

| Run No. | Block | Acid concentration (M) | Temperature (°C) | L/S (mL/g) | Time (h) | Actual recovery of vanadium (%)[a] | Predicted recovery of vanadium (%) |
|---|---|---|---|---|---|---|---|
| 1 | Axial | 4.0 | 80.0 | 20.0 | 4.5 | 77.3 ± 1.2 | 75.0 |
| 2 | Fact | 3.0 | 85.0 | 16.2 | 3.7 | 78.2 ± 0.9 | 79.0 |
| 3 | Axial | 6.0 | 80.0 | 12.5 | 4.5 | 82.4 ± 0.4 | 80.1 |
| 4 | Center | 4.0 | 80.0 | 12.5 | 4.5 | 86.1 ± 1.0 | 85.0 |
| 5 | Fact | 5.0 | 85.0 | 8.7 | 5.2 | 81.2 ± 0.5 | 82.0 |
| 6 | Axial | 4.0 | 80.0 | 5.0 | 4.5 | 77.0 ± 1.3 | 76.0 |
| 7 | Center | 4.0 | 80.0 | 12.5 | 4.5 | 83.7 ± 0.6 | 85.0 |
| 8 | Fact | 5.0 | 75.0 | 16.2 | 5.2 | 77.2 ± 0.9 | 78.0 |
| 9 | Fact | 3.0 | 75.0 | 8.7 | 3.7 | 72.8 ± 1.0 | 73.1 |
| 10 | Fact | 3.0 | 75.0 | 16.2 | 3.7 | 72.0 ± 1.4 | 72.0 |
| 11 | Fact | 3.0 | 85.0 | 8.7 | 3.7 | 78.2 ± 0.5 | 79.0 |
| 12 | Fact | 5.0 | 75.0 | 8.7 | 3.7 | 77.2 ± 1.5 | 77.0 |
| 13 | Fact | 3.0 | 85.0 | 16.2 | 5.2 | 79.1 ± 1.9 | 80.0 |
| 14 | Fact | 5.0 | 85.0 | 16.2 | 3.7 | 79.5 ± 1.2 | 81.0 |
| 15 | Fact | 3.0 | 85.0 | 8.7 | 5.2 | 80.0 ± 1.1 | 80.1 |
| 16 | Axial | 4.0 | 70.0 | 12.5 | 4.5 | 74.0 ± 0.9 | 74.0 |
| 17 | Fact | 3.0 | 75.0 | 8.7 | 5.2 | 74.0 ± 0.8 | 74.0 |
| 18 | Fact | 5.0 | 85.0 | 8.7 | 3.7 | 80.0 ± 0.8 | 81.0 |
| 19 | Axial | 2.0 | 80.0 | 12.5 | 4.5 | 74.2 ± 0.6 | 73.0 |
| 20 | Fact | 5.0 | 75.0 | 16.2 | 3.7 | 75.0 ± 0.6 | 76.0 |
| 21 | Center | 4.0 | 80.0 | 12.5 | 4.5 | 86.0 ± 0.5 | 85.0 |
| 22 | Fact | 5.0 | 75.0 | 8.75 | 5.2 | 78.3 ± 0.5 | 78.0 |
| 23 | Fact | 5.0 | 85.0 | 16.2 | 5.2 | 81.0 ± 0.9 | 82.0 |
| 24 | Center | 4.0 | 80.0 | 12.5 | 4.5 | 85.0 ± 0.9 | 85.0 |
| 25 | Center | 4.0 | 80.0 | 12.5 | 4.5 | 84.1 ± 0.5 | 85.0 |
| 26 | Fact | 3.0 | 75.0 | 16.2 | 5.2 | 73.0 ± 0.8 | 73.0 |
| 27 | Axial | 4.0 | 90.0 | 12.5 | 4.5 | 87.4 ± 0.4 | 85.0 |
| 28 | Axial | 4.0 | 80.0 | 12.5 | 6.0 | 83.0 ± 0.6 | 82.0 |
| 29 | Axial | 4.0 | 80.0 | 12.5 | 3.0 | 80.3 ± 1.1 | 79.0 |
| 30 | Center | 4.0 | 80.0 | 12.5 | 4.5 | 84.0 ± 0.8 | 85.0 |

[a]Mean ± standard deviation.

## 3. Results and discussion
### 3.1. Magnetite ore characterization
The XRD pattern of the magnetite ore and the major minerals that were present in the sample are shown in Figure 1. The XRD results revealed that the major phases in the sample were magnetite ($Fe_3O_4$) 67(wt%), talc ($Mg_3(Si_4O_{10})(OH)_2$) 13(wt%), serpentine (antigorite) ($Mg_6(Si_4O_{10})(OH)_8$) 10(wt%), pyrite ($FeS_2$) 6(wt%), and chlorite ($(Mg,Fe)_{4.75}Al_{1.25}(Al_{1.25}Si_{2.75}O_{10})(OH)_8$) 4(wt%). Also according to the mineralogical studies of thin and more polished sections (Figure 2), opaque (magnetite), carbonate, talc, iron oxides and hydroxide minerals were observed in the sample.

Table 1 presents the results of a chemical analysis of the sample with respect to the XRF results. As it can be seen, the sample contained 0.63% $V_2O_5$, which was equivalent to 0.35% vanadium. Also the magnetite ore contained alkaline metal oxides, specifically a large amount of iron oxide, which resulted in the strong magnetite property of the sample.

The XRD analysis obtained after the roasting process is presented in Figure 3. The XRD results revealed that the major phases in the roasted ore were magnetite ($Fe_3O_4$), cristobalite ($SiO_2$), maghemite ($Fe_2O_3$), magnesium aluminum iron oxide ($MgAl_2Fe_{1.8}O_4$), metavanadate sodium ($NaVO_3$), and sodium magnesium aluminum silicate ($Na_{1.74}Mg_{0.79}Al_{0.15}Si_{1.06}O_4$) dispersed in a low-intensity pattern. Comparing Figs. 1 and 3 shows that after roasting, a more water-soluble vanadium ($NaVO_3$) is obtained [2].

### 3.2. Optimization of roasting parameters

Ranges and levels of the variables in coded units summarized in Tables 2 and 5 show the actual values for three independent variables together with the responses.

### 3.2.1 Model fitting and analysis of variance (ANOVA)
Table 7 reports the results of the ANOVA test performed using the DX8 program for the roasting process. This statistical tool was used to examine the significance and adequacy of the model. This table presents that the correlation coefficient for the model is 0.94, which indicates the goodness of fit. Table 7 also reports that the calculated F-value corresponding to the vanadium recovery response model is 5.95 and exceeds the value at the 5% level, indicating that the treatment differences are highly significant. The probability P-value is relatively low, indicating the significance of the model.

In order to estimate the model coefficients and the response for the quadratic polynomial, multiple regression analysis of the experimental data was employed and the following equation was obtained:

$$\text{Recovery (\%)} = 85.46 + 1.53\,A + 0.88\,B + 0.98C - 0.25AB - 1.00AC + 0.75BC - 4.21A^2 - 4.12B^2 - 3.06C^2 \tag{3}$$

where A, B, and C are the coded values of the test variables, temperature (A) in °C, time (B) in h, and salt content (C) in wt%. In this regard, the perturbation diagram reveals that temperature and time are the most and least effective parameters, respectively.

**Table 7. Results of ANOVA for the roasting process.**

| Source | Sum of squares | DF | Mean square | F-value | P-value prob > F | Adj R-squared | R-squared | Adeq. precision |
|---|---|---|---|---|---|---|---|---|
| Model | 602.65 | 9 | 66.96 | 5.95 | 0.0050 | 0.84 | 0.94 | 16.45 |
| A: Temperature | 32.08 | 1 | 32.08 | 2.85 | 0.0122 | | | |
| B: Time | 10.54 | 1 | 10.54 | 0.94 | 0.0356 | | | |
| C: Salt content | 13.08 | 1 | 13.08 | 1.16 | 0.0306 | | | |
| AB | 0.5 | 1 | 0.50 | 0.044 | 0.0084 | | | |
| AC | 8.00 | 1 | 8.00 | 0.71 | 0.0419 | | | |
| BC | 4.50 | 1 | 4.50 | 0.40 | 0.0541 | | | |
| $A^2$ | 255.73 | 1 | 255.73 | 22.73 | 0.0008 | | | |
| $B^2$ | 245.11 | 1 | 245.11 | 21.79 | 0.0009 | | | |
| $C^2$ | 135.25 | 1 | 135.25 | 12.02 | 0.0060 | | | |
| Residual | 112.48 | 10 | 11.25 | | | | | |
| Lack-of-fit | 67.15 | 5 | 13.43 | 1.48 | 0.3384 | | | |
| Pure error | 45.33 | 5 | 9.07 | | | | | |
| Total | 715.14 | 19 | | | | | | |

### 3.2.2. Response surface plotting

In order to study the model more thoroughly, the results obtained are presented graphically in Figs. 4 and 5. Interaction terms with small P-value (less than 0.05) and the largest absolute coefficients in the fitted model (AB (temperature × time) and AC (temperature × salt content)) were selected for the axes of the response surface plots to account for the curvature of the surfaces. The interaction implies that the effect produced via changing one variable depends on the level of the other variables. In vanadium recovery, temperature (A), and salt content (C) are significant variables affecting the vanadium yield response. The interactions between the parameters are shown in Figure 4.

Figure 4a shows the interaction between time and temperature. As shown in this figure, at certain times, with the temperature rising up to 1000 °C, the vanadium yield increases and decreases, probably due to the sample sintering at above 1000 °C. Also it can be seen that at a higher period (2.6 h), the efficiency of vanadium is more than that at a lower period (1.4 h). In this case, the salt content for roasting is 40 (wt%). With regard to this figure, temperature plays an important role in the roasting process. By increasing the temperature to a certain amount, the sodium methavanadate compound is further produced so that vanadium can be easily extracted from the roasted ore.

Figure 4b shows the interaction between the salt content and temperature. Based on this figure, at a higher salt content (46 wt%), the efficiency of vanadium extraction is higher than that at a lower salt content (34 wt%), and with raising the temperature up to 1000 °C, the vanadium extraction is improved, and decreases slightly

thereafter. As seen at a higher temperature (~1100 °C), the same recovery of vanadium is obtained for two salt contents (34 and 46 wt%). In this case, the roasting time is 2 h. Thus after the temperature, the amount of salt consumed has an important effect on the vanadium extraction efficiency. Moreover, according to Figure 4, at very high temperatures, differences in the amounts of salt consumed have no significant effect on the efficiency of vanadium extraction.

Figure 5 shows the second-order iso-response contours for the vanadium recovery percentage varying as a function of the temperature and the salt content, where the time was set to 2 h. There is a nearly linear relationship between vanadium recovery and salt content at low temperatures. However, at a higher temperature, the relationship becomes a non-linear one. As presented in this figure, the highest vanadium recovery corresponds to a high temperature of 1000 °C and salt content of 40 wt%. As illustrated in this figure, at low temperatures (less than 950 °C), low salt contents (below 35 wt%), very high temperatures (> 1050 °C), and very high salt contents (> 45 wt%), the vanadium extraction efficiency decreases. This figure also shows the effects of two important parameters of temperature and amount of salt consumed simultaneously on the vanadium extraction efficiency from roasted ore. By increasing the temperature and amount of salt to a certain amount, vanadium will be extracted with a maximum efficiency.

Figure 6 shows the 3D effects of temperature and amount of salt on the extraction efficiency of vanadium. As shown in this figure, the maximum vanadium extraction efficiency occurs at a temperature of 1000 °C and the salt amount of 40 wt%, while the roasting time is 2 h.
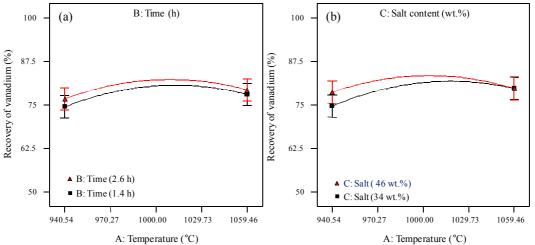


**Figure 4. (a) Interaction between temperature and time and (b) interaction between temperature and salt content.**
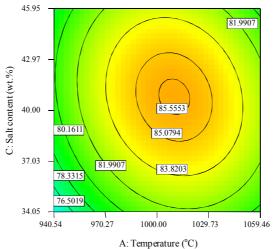
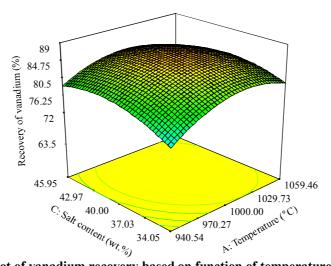**Figure 5. Contour plot of vanadium recovery *vs.* temperature and salt content.**



**Figure 6. A 3D plot of vanadium recovery based on function of temperature and salt content.**

### 3.2.3. Process optimization using desirability functions

A multiple response method was applied to optimize any combination of three parameters, namely temperature, salt content, and time. According to the desirability ramp generated from 20 local optimum points, the best local maximum (vanadium recovery of 85.7%) was found to be attributed to the temperature of 1009 °C, salt content of 40.88 wt%, and time of 2.07 h. In order to test the validity of the optimized condition specified by the model, an experiment was carried out using the suggested parameters. The vanadium recovery after the leaching period was determined to be 83.4%, which is consistent with the prediction of the model with an error margin of 2.7% (< 5%). The leaching conditions used in the confirmatory experiment were as follow: temperature of 90 °C, acid concentration of 4 M, L/S ratio of 10 mL/g, and leaching time of 4 h.

### 3.3. Optimization of leaching parameters

The ranges and levels of the variables in coded units summarized in Tables 3 and 6 show the actual values for the four independent variables together with their responses.

### 3.3.1. Model fitting and ANOVA

Table 8 presents the results of the ANOVA test performed using the DX8 program for the leaching process. This statistical tool was used to examine the significance and adequacy of the model. It can be seen in this table that the correlation coefficient for the model is 0.918, which indicates the goodness of fit. Table 8 also reports that the calculated F-value corresponding to the vanadium recovery response model is 12.00 and exceeds the value at the 5% level, implying that the treatment differences are highly significant. Also the P-value is relatively low, indicating the significance of the model. By implementing the multiple regression analysis of the experimental data, the experimental results for CCD were fitted with a quadratic polynomial

equation. The final equation in terms of coded factors was developed based on the experimental design as:

$$\text{Recovery (\%)} = 84.67 + 1.54A + 2.71B - 0.29C + 0.71D - 0.56AB - 0.062AC + 0.063AD + 0.19BC + 0.063BD + 0.063CD - 2.03A^2 - 1.28B^2 - 2.28C^2 - 1.16D^2 \quad (4)$$

where A, B, C, and D are the coded values of the test variables, acid concentration (A) in M, temperature (B) in °C, L/S (C) in mL/g, and time (D) in h. The perturbation diagram and the above

equation revealed that temperature was the most effective parameter, while the liquid-to-solid ratio (L/S) was the least effective influencing parameter. Figure 7 presents the actual values versus the predicted ones for vanadium recovery. As shown in in this figure, the assembly of the points around the diagonal line illustrates that the experimental results are in good agreement with the predicted values, and, therefore, the deviations between the predicted values and the actual values are very small.

**Table 8. ANOVA results for the leaching process.**

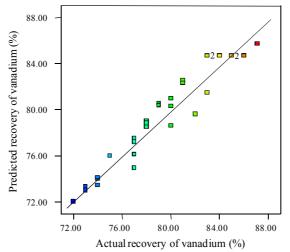| Source | Sum of squares | DF | Mean square | F-value | P-value | Adj R-squared | R-squared | Adeq. precision |
|---|---|---|---|---|---|---|---|---|
| Model | 501.12 | 14 | 35.79 | 12.00 | <0.0001 | 0.842 | 0.918 | 12.57 |
| A: H$_2$SO$_4$ | 57.04 | 1 | 57.04 | 19.12 | 0.0005 | | | |
| B: Temperature | 176.04 | 1 | 176.04 | 59.01 | <0.0001 | | | |
| C: L/S | 2.04 | 1 | 2.04 | 0.68 | 0.0421 | | | |
| D: Time | 12.04 | 1 | 12.04 | 4.04 | 0.0462 | | | |
| AB | 5.06 | 1 | 5.06 | 1.70 | 0.0212 | | | |
| AC | 0.063 | 1 | 0.063 | 0.021 | 0.0089 | | | |
| AD | 0.063 | 1 | 0.063 | 0.021 | 0.0089 | | | |
| BC | 0.56 | 1 | 0.56 | 0.19 | 0.0067 | | | |
| BD | 0.063 | 1 | 0.063 | 0.021 | 0.0089 | | | |
| CD | 0.063 | 1 | 0.063 | 0.021 | 0.0089 | | | |
| A$^2$ | 113.17 | 1 | 113.17 | 37.93 | <0.0001 | | | |
| B$^2$ | 45.03 | 1 | 45.03 | 15.09 | 0.0015 | | | |
| C$^2$ | 142.74 | 1 | 142.74 | 47.85 | <0.0001 | | | |
| D$^2$ | 36.67 | 1 | 36.67 | 12.29 | 0.0032 | | | |
| Residual | 44.75 | 15 | 2.98 | | | | | |
| Lack-of-fit | 37.42 | 10 | 3.74 | 2.55 | 0.1565 | | | |
| Pure error | 7.33 | 5 | 1.47 | | | | | |
| Total | 545.87 | 29 | | | | | | |



**Figure 7. Comparison of the actual and predicted values for vanadium recovery.**

### 3.3.2. Response surface plotting

For a better understanding of the independent parameters and their influence on the recovery of vanadium, the predicted results are presented graphically in Figures 8 and 9. Interaction terms with P-value < 0.05 and largest absolute

coefficients in the fitted model (AB (acid concentration × temperature), AC (acid concentration × L/S), and BC (temperature × L/S)) were selected for the axes of the response surface plots to account for the curvature of the surfaces. In the recovery of vanadium, A (acid

concentration), B (temperature), C (L/S), and D (time) are significant variables affecting the response. The interactions between the parameters are presented in Figure 8.

Figure 8a shows the interaction between the acid concentration and temperature. As shown in this figure, the vanadium extraction efficiency at a higher temperature exceeds the one at a lower temperature in all acid concentrations. At a constant temperature, by increasing the concentration of acid until 4.25 M, the vanadium efficiency will increase and can even decrease thereafter probably due to the higher concentration of $H_2SO_4$, leading to more aluminosilicate reacting with $H_2SO_4$ to produce a silica gel, which can adsorb the positive cations of vanadium such as $VO^{+2}$ and $VO_2^+$.

Figure 8b shows the interaction between the acid concentration and L/S. Based on this figure, the vanadium extraction efficiency in all acid concentrations at a lower liquid-to-solid ratio (L/S = 8.75) is more than that of a higher

liquid-to-solid ratio (L/S = 16.25). Moreover, their efficiency difference is not too much in different acid concentrations. For a constant L/S, with an increase in acid concentration up to a certain value (4.25 M), the vanadium extraction efficiency increases and reduces thereafter.

Figure 8c shows the interaction between L/S and temperature. As seen at low temperatures, the less the liquid-to-solid ratio (L/S = 8.75), the more is the extraction efficiency of vanadium. At high temperatures, these two efficiencies (with different L/S) are close together.

Figure 9 shows the 3D effects of temperature, acid concentration, and L/S on the extraction efficiency of vanadium. As presented in Figure 9a, with an increase in temperature and reducing L/S until 12.5, the vanadium extraction efficiency increases. Also based on Figure 9b, as acid concentrations increase until 4.25 M, L/S reduces until 12.5 along with an increase in the vanadium extraction efficiency.
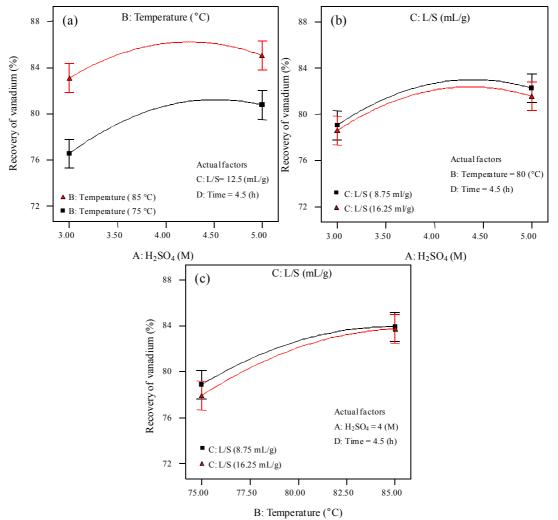


**Figure 8. (a) Interaction between acid concentration and temperature, (b) Interaction between acid concentration and L/S, and (C) Interaction between temperature and L/S.**
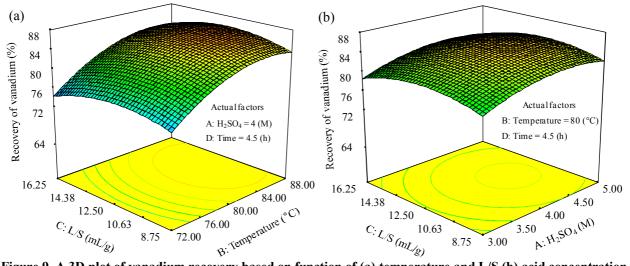
**Figure 9. A 3D plot of vanadium recovery based on function of (a) temperature and L/S (b) acid concentration and L/S.**

### 3.3.3. Process optimization using desirability functions

A multiple response method was used to optimize any combination of four parameters, namely acid concentration, temperature, L/S, and time. According to the desirability ramp generated from 30 local optimum points, the best local maximum was found to be at the acid concentration of 4.25 M, the temperature of 85 °C, a liquid-to-solid ratio of 12.4 mL/g, and time of 4.7 h, which resulted in a vanadium recovery of 86.34%. In order to test the validity of the optimized conditions specified by the model, an experiment was carried out using the suggested parameters. The vanadium recovery after the leaching period was determined to be 83.8%, which is consistent with the prediction of the model with an error margin of 2.9% (< 5%). The conditions of the roasting process used in the confirmatory experiment were as follow: temperature of 1000 °C, the salt content of 40 wt%, and time of 2 h.

The comparisons between the vanadium recoveries obtained from the present work and those reported in the literature are presented in Table 9. It can be seen that under the optimal conditions, recovery of vanadium from magnetite ore of Saghand mine is reasonably improved.

**Table 9. Comparison of vanadium recovery obtained from various resources.**

| Resources | Vanadium (wt%) | Methods | Conditions | Recovery (%) | References |
|---|---|---|---|---|---|
| Ore | 0.52 | Roasting-acid leaching | Roasting: 950 °C, 1 h; leaching: sulfuric acid (0.45%), 30 °C | More than 76% | [20] |
| Ore | 1.06 | Roasting-alkaline leaching | Roasting: 850 °C, 3h; leaching: NaOH (2 M), 90 °C | More than 67% | [21] |
| Slag | 1.09 | Roasting-acid leaching | Roasting: 1000 °C, 2 h; leaching: sulfuric acid (2 M), 70 °C | More than 96% | [33] |
| Ore | 0.4 | Roasting-acid leaching | Roasting: 900 °C, 2 h; leaching: sulfuric acid (4 M), 90 °C | More than 70% | [17] |
| Slag | 1.15 | Roasting-acid leaching | Roasting: 1000 °C, 2 h; leaching: sulfuric acid (3 M), 70 °C | More than 95% | [22] |
| Slag | 4.46 | Roasting-acid leaching | Roasting: 850 °C, 2 h; leaching: sulfuric acid (15% vol.), 90 °C | More than 93% | [34] |
| Ore (Saghand-e-Yazed mine) | 0.35 | Roasting-acid leaching | Roasting: 1000 °C, 2 h; leaching: sulfuric acid (4.25 M), 85 °C | More than 83% | This work |

### 3.3.4. Characterization of leach residue

To understand the mechanism of the vanadium leaching process, the leach residues were analyzed through SEM and EDS under the optimum conditions. Figures 10a and 10b show the SEM/EDS results for a residue sample. These regions are mainly composed of iron, oxygen, sulfur, and silica, while only very low amounts of vanadium are present. Accordingly, the magnetite and maghemite were decomposed by alkaline roasting and sulfuric acid leaching, leading to the vanadium release from the ore. Therefore, to improve the vanadium recovery, the decomposition of the vanadium-iron spinel is required. These results are consistent with the XRF results.
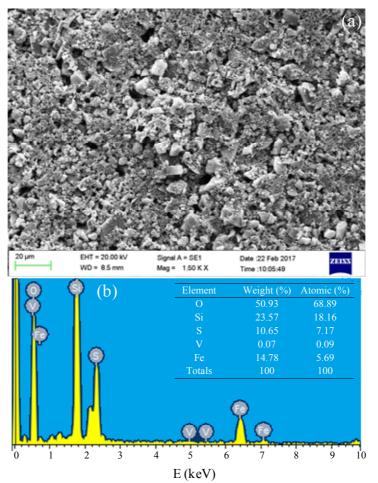


| Element | Weight (%) | Atomic (%) |
|---------|-----------|-----------|
| O | 50.93 | 68.89 |
| Si | 23.57 | 18.16 |
| S | 10.65 | 7.17 |
| V | 0.07 | 0.09 |
| Fe | 14.78 | 5.69 |
| Totals | 100 | 100 |

E (keV)

**Figure 10. SEM-BSE image (a) and EDS (b) of the leach residue.**

### 4. Conclusions

Based on the results obtained from the current research work, the following conclusions were drawn:

1. The sample contained 0.35% vanadium. The magnetite ore sample was alkaline-roasted to increase the solubility of the vanadium compound.

2. From the XRD results, the alkaline-roasting process converted part of the sample to sodium vanadate ($NaVO_3$), which was more soluble in acid leaching.

3. To optimize the values for temperature, sodium carbonate content, and time in the roasting process, the CCD response surface methodology was used. The most effective and the least effective parameters were found to be temperature and time, respectively.

4. Optimizing the leaching parameters through the above-mentioned method revealed that the most and least effective parameters were temperature and L/S, respectively.

5. The optimum temperature, sodium carbonate content, and time in the roasting process based on RSM were 1010 °C, 41 wt%, and 2.1 h, respectively.

6. Based on RSM, the best local maximum for the leaching process was found to be a temperature of 85 °C, a sulfuric acid concentration of 4.25 M, an L/S ratio of 12.4 mL/g, and a time of 4 h. According to the prediction of the model,

86.34% of vanadium could be extracted from the ore.

7. Under the optimum conditions, more than 83% of vanadium was leached from the magnetite ore.

## Acknowledgments

## References

[1]. Moskalyk, R.R. and Alfantazi, A.M. (2003). Processing of vanadium: a review. Miner. Eng. 16 (9): 793-805.

[2]. Gupta, C.K. and Krishnamurthy, N. (1992). Extractive Metallurgy of Vanadium. Elsevier, Amsterdam, New York.

[3]. Ullmann, F. (1998). Ullmans Encyclopedia of Industrial Chemistry, 6th ed., Weinheim, Germany.

[4]. Habashi, F. (1997). Handbook of Extractive Metallurgy. vol. 3, Wiley-VCH, Heidelberg, Germany.

[5]. Chen, X.Y., Lan, X.Zh., Zhang, Q.L., Ma, H.Zh. and Zhou, J. (2010). Leaching vanadium by high concentration sulfuric acid from stone coal. Trans. Nonferr. Metal Soc. china. 20: 123-126.

[6]. Habashi, F. (1969). Principles of Extractive Metallurgy, vol. 1: General Principles, Gordon and Breach, New York.

[7]. Li, C.X., Wei, C.H., Deng, Zh.G., Li, M.T., Li, X.B. and Fan, G. (2010). Recovery of vanadium from black shale. Trans. Nonferr. Metal Soc. china. 20: 127-131.

[8]. Amer, A.M. (2002). Processing of Egyptian boiler ash for extraction of vanadium and nickel. Waste Manage. 22 (5): 515-520.

[9]. Navarro, R., Guzman, J., Saucedo, I., Revilla, J. and Guibal, E. (2007). Vanadium recovery from oil fly ash by leaching precipitation and solvent extraction processes. Waste Manage. 27 (3): 425-438.

[10]. Murase, K., Nishikawa, K.I., Ozaki, T., Machida, K.I., Adachi, G.Y. and Suda, T. (1998). Recovery of vanadium, nickel and magnesium from a fly ash of bitumen-in-water emulsion by chlorination and chemical transport. J. Alloys compd. 264 (1-2): 151-156.

[11]. Vitolo, S., Seggiani, M., Filippi, S. and Brocchini, C. (2000). Recovery of vanadium from heavy oil and Orimulsion fly ashes. Hydrometallurgy. 57 (2): 141-149.

[12]. Wilkomirsky, I.A.E., Luraschi, A. and Reghezza, A. (1985). Vanadium extraction process from basic steel refining slags. A. Extraction metallurgy 85, The Institution of Mining and Metallurgy, London. pp. 531-549.

[13]. Voglauer, B., Grausam, A. and Jorgel, H.P. (2004). Reaction-kinetics of the vanadium roast process using steel slag as a secondary raw material. Miner. Eng. 17 (2): 317-321.

[14]. Jin, X.Zh. (2000). Phase analysis of vanadium in carbonaceous shale. Chin. J. Anal. Lab. 19 (2): 50-52.

[15]. He, D., Feng, Q., Zhang, G., Luo, W. and Ou, L. (2008). Study on leaching vanadium from roasting residue of stone coal. Miner. Metall. Process. 25 (4): 181-184.

[16]. Jena, B.C., Dresler, W. and Reilly, L.G. (1995). Extraction of titanium, vanadium and iron from titanomagnetite deposits at pipestone lake. Monitoba, Canada, Miner. Eng. 8 (1-2): 159-168.

[17]. Hu, Y.J., Zhang, Y.M., Bao, Sh.X. and Liu, T. (2012). Effects of the mineral phase and valence of vanadium on vanadium extraction from stone coal. Int. J. Mine Metall. Mater. 19 (10): 893-898.

[18]. Gabra, G. and Malinsky, I. (1980). A comparative study of the extraction of vanadium from titaniferous magnetites. Extr. Metall. Refract. Metals, Metallurgical Society of AIME. pp. 167-189.

[19]. Li, X.Sh., Xie, B., Wang, G.E. and Li, X.J. (2011). Oxidation process of low-grade vanadium slag in presence of $Na_2CO_3$. Trans. Nonferr. Met. Soc. China. 21 (8): 1860-1867.

[20]. Zhu, Y.G., Zhang, G.F., Feng, Q.M., Lu, Y.P., Ou, L.M. and Huang, S.J. (2010). Acid leaching of vanadium from roasted residue of stone coal. Trans. Nonferr. Met. Soc. China. 20: 107-111.

[21]. He, D., Feng, Q., Zhang, G., Ou, L. and Lu, Y. (2007). An environmentally friendly technology of vanadium extraction from stone coal. Miner. Eng. 20 (12): 1184-1186.

[22]. Aarabi-Karasgani, M., Rashchi, F., Mostoufi, N. and Vahidi, E. (2010). Leaching of vanadium from LD converter slag using sulfuric acid. Hydrometallurgy. 102 (1-4): 14-21.

[23]. Montgomery, D.C. (2008). Design Analysis of Experiments, 7th ed., Wiley, New York.

[24]. Garcia-Diaz, A. and Philips, D.T. (1994). Principles of Experimental Design and Analysis, Springer, Chapman and Hall, London.

[25]. Correia, D.S., Gonçalves, C.V., da Cunha Jr, S.S. and Ferraresi, V.A. (2005). Comparison between genetic algorithms and response surface methodology in GMAW welding optimization. J. Mater. Process Technol. 160 (1): 70-76.

[26]. Erzurumlu, T. and Orkem, H. (2007). Comparison of response surface model with neural network in determining the surface quality of moulded parts. Mater. Des. 28 (2): 459-465.

[27]. Hamzaoui, A.H., Jamoussi, B. and M'nif, A. (2008). Lithium recovery from highly concentrated solution: response surface methodology (RSM) process parameters optimization. Hydrometallurgy. 90 (1): 1-7.

[28]. Myers, R.H., Montgomery, D.C. and Anderson-Cook, C.H.M. (2016). Response Surface Methodology: Process and Product Optimization Using Designed Experiments. 4th ed., Wiley, New York.

[29]. Zare Tavakoli, H., Abdollahy, M., Ahmadi, S.J. and Khodadadi Darban, A. (2017). Enhancing recovery of uranium column bioleaching by process optimization and kinetic modeling. Trans. Nonferr. Met. Soc. 27: 2691-2703.

[30]. Li, M., Wei, C.H., Fan, G., Wu, H., Li, C. and Li, X. (2010). Acid leaching of black shale for the extraction of vanadium. Int. J. Miner. process. 95 (1-4): 62-67.

[31]. Naseri Joda, N. and Rashchi, F. (2012). Recovery of ultra fine grained silver and copper from PC board scraps. Sep. Purif. Technol. 92: 36-42.

[32]. Amiri, F., Mousavi, S.M. and Yaghmaei, S. (2011). Enhancement of bioleaching of a spent Ni/Mo hydroprocessing catalyst by Penicillium simplicissimum. Sep. Purif. Technol. 80 (3): 566-576.

[33]. Mirazimi, S.M.J., Rashchi, F. and Saba, M. (2013). Vanadium removal from roasted LD converter slag: optimization of parameters by response surface methodology (RSM). Sep. Purif. Technol. 116: 175-183.

[34].Yang, Z., Li, H.Y., Yin, X.C., Yan, Z.M., Yan, X.M. and Xie, B. (2014). Leaching kinetics of calcification roasted vanadium slag with high CaO content by sulfuric acid. Int. J. Miner. process. 133: 105-111.

# استخراج وانادیوم از کانسنگ مگنتیتی با استفاده از فرآیندهای تشویه و فروشویی اسیدی: بهینه‌سازی پارامترهای فرآیندی به وسیله روش سطح پاسخ

داود قدوسی‌نژاد¹، مجید تقی‌زاده*۱ و علیرضا خانچی²

۱- دانشکده‌ی مهندسی شیمی، دانشگاه صنعتی نوشیروانی بابل، ایران

۲- پژوهشکده‌ی مواد و سوخت هسته‌ای، پژوهشگاه علوم و فنون هسته‌ای، سازمان انرژی اتمی، ایران

* نویسنده مسئول مکاتبات: taghizadeh@nit.ac.ir

## چکیده:

در این پژوهش، فرآیندهای تشویه قلیایی و فروشویی اسید سولفوریکی برای استخراج وانادیوم از کانسنگ مگنتیتی معدن ساغند در ایران مرکزی اسـتفاده شـده است. روش سطح پاسخ بر اساس مدل طراحی ترکیبی مرکزی برای بهینه‌سازی پارامترهای فرآیندی به کار رفته است. پارامترهای تشویه تحقیق شده شامل درجه حرارت (۹۰۰-۱۱۰۰ درجه سانتی‌گراد)، کربنات سدیم (۳۰-۵۰ درصد وزنی) و زمان (۱-۳ ساعت) بوده است. به علاوه فاکتورهای فروشویی مورد مطالعه شـامل درجه حرارت (۷۰-۹۰ درجه سانتی‌گراد)، نسبت مایع به جامد (۵-۲۰ گرم/میلی‌لیتر)، غلظت اسید سولفوریک (۲-۶ مولار) و زمان (۳-۶ ساعت) بوده است. تحت شرایط بهینه، مقادیر درجه حرارت، زمان و کربنات سدیم در فرآیند تشویه به ترتیب شامل ۱۰۱۰ درجه سانتی‌گراد، ۲/۱ ساعت و ۴۱ درصد وزنی بوده، در حالی که مقادیر درجه حرارت، نسبت مایع به جامد، غلظت اسید سولفوریک و زمان در فرآیند فروشویی شامل ۸۵ درجه سانتی‌گراد، ۱۲/۴ گرم/میلی‌لیتر، ۴/۲۵ مولار و ۴/۷ ساعت تعیین شده است. تحت این شرایط بهینه، ۸۳/۸ ±۰/۸۷ درصد وانادیوم از کانسنگ مگنتیتی استخراج شده است.

**کلمات کلیدی:** کانسنگ مگنتیتی، وانادیوم، تشویه قلیایی، فروشویی اسیدی، بهینه‌سازی.